2-D modelling of effect of free-stream turbulence on trailing edge vortex

IOP Conf. Series: Materials Science and Engineering **909** (2020) 012039 doi:10.1088/1757-899X/909/1/012039

2-D modelling of effect of free-stream turbulence on trailing edge vortex

Syaiful[1*], Anggie Restue Saputra[1], Nazaruddin Sinaga[1] and Bambang Yunianti[1]
[1]Departement of Mechanical Engineering, Diponegoro University, Semarang, Indonesia

[*]Email: syaiful.undip2011@gmail.com

Abstract Vorticity causes many adverse effects on the area near the surface, both on moving (turbine blade) and fixed objects. Therefore, this study attempts to investigate the effects of free-stream turbulence on trailing edge vortex on the NACA 0015 airfoil profile. This research was conducted using two-dimensional numerical simulations. To determine the interaction of vortex and free stream turbulence, two variations of turbulent intensity were given, namely 0.5% and 4.6% with Reynolds number of 1.6 x 10^5. The k-ε turbulence model was used in the current study. The angle of attack of the flow towards the airfoil was varied from 0° to 25° in conditions of increase and decrease in the horizontal position of the airfoil. The result was found that there is an agreement between the simulation and the experiment result. Increased turbulent intensity can delay the stall condition, the stall process begins to be observed after the 12° attack angle at 0.5% turbulent intensity while at turbulent intensity 4.6% the stall process was found after the 15° attack angle. From a velocity streamline, it was found that an increase in turbulent intensity can inhibit vortex growth.

1. Introduction

According to the projection of the International Energy Agency (IEA), up to 2030 world energy demand has increased by 45% or an average increase of 1.6% per year. Most or about 80% of the world's energy needs are supplied from fossil fuels [1]. Therefore, the use of new renewable energy needs to be improved. The wind is one of the potential energy sources that can be used as renewable energy. Wind turbines utilize mechanical energy from the wind to produce electrical power [2]. One crucial part of a wind turbine is the blade because this part is directly related to the flow of wind. The wind turbine blade has a particular blade profile called an airfoil that determines the primary performance of the wind turbine [3].

Various flow phenomena are found around the blade, including vortices. Vorticity can also be found in a variety of practical aerodynamic applications, such as wind turbine [4]. When the wind turbine rotates because of the fluid flow around it, vortices are generated. Vorticity causes many adverse effects on the near-field surface, both rotating and immovable objects [5]. The disadvantages caused by these vortices include high noise, vibration, mechanical fatigue, and erosion. These losses can occur in aerodynamically shaped objects, such as aircraft wings, helicopter propellers, ship propellers, and wind turbine blades.

Flow conditions and surface geometry influence the process of vortex formation. Reynolds number, flow attack angle, turbulent boundary layer, aspect ratio, and geometry of the surface are the parameters

that affect the vortex formation process [6]. The method of formation, structure, and shape change of the vortex has been extensively studied. Meanwhile, vortex interaction with external disorders has not received much attention. Free-stream turbulence is an example of an external disorder that can affect vorticity [7].

Several studies have discussed the airfoil, vortex, and the effects of free-stream turbulence. Maldonado et al. (2015) conducted a review of the impact of free-stream turbulence on the aerodynamic performance of type S809 wind turbine blades with variations without and with turbulent grids (TU = 6.14%) [8]. From testing Maldando et al. (2015) note that an increase in turbulent intensity can increase the lift to drag (L/D) ratio and delay flow separation at high attack angles. The effect of turbulent intensity on the aerodynamic performance of horizontal wind turbines has been studied by Li et al.[9]. The results of their study indicated that an increase in turbulent intensity increases the lift coefficient at an angle of attack between 0° to 20°. Kim and Xi (2016) investigated the effect of turbulent intensity on the stall condition on the wind turbine blade [10]. They revealed that dynamic stall on the blade is generally found at an angle of attack greater than 18. Increased turbulent intensity from 0 to 10% results in an increase in the lift coefficient and drag coefficient at the angle of attack from 4° to 20°. Yao et al. (2012) studied numerically by comparing several turbulent models namely k-ε, RNG k-ε, SST4 model, Reynolds model [11]. Yao et al. observed that the lift coefficient from the numerical simulation results on all turbulent models had values that approached the experimental data. The effect of free-stream turbulence on the dynamic stall from wind turbine blades has been investigated by Kim and Xie (2016) [12]. Kim and Xie (2016) revealed that higher turbulent intensity reduces bubble separation, which causes an increase in the ratio of lift to drag (L/D) on static airfoils. Ahmadi-Baloutaki et al. (2015) investigated experimentally about the interaction of free-stream turbulence against near-field wing-tip vortex [7]. Ahmadi-Baloutaki et al. found that increasing turbulent intensity could increase the near-field wing-tip vortex decay rate and improve aerodynamic performance with static stall delay.

From previous studies, it can be seen that most of the results of the study reveal that free-stream turbulence can delay stall conditions. However, studies that focus on discussing the effects of free-stream turbulence on vortex that appear around the wings or blade on the turbine are very few. Therefore, the present study aims to discuss in detail the effect of free-stream turbulence on trailing edge vortex with a two-dimensional numerical simulation on the profile of the NACA 005 airfoil.

2. Description Of Physical Model

The profile of the NACA 0015 airfoil was used in this study. The NACA airfoil profile was developed by the U.S. National Aviation Advisory Board [11]. The airfoil profile used has a geometry with a chord length of 0.152 m, as can be seen in Figure 1. This airfoil has a symmetrical geometry with a maximum thickness of 15% of the length of the chord. The geometry used in this numerical simulation was the same as that used in Ahmad-Baloutaki et al. [7].

The numerical simulation parameter is determined by the Reynolds number: $Re = \rho uc/\mu$, where ρ is the air density, $\rho = 1{,}225$ kg/m^3; μ is dynamic viscosity, $\mu = 1.7894 \times 10^{-5}$ kg/ms; c is the chord length of the airfoil, u is the velocity of fluid flow. The Reynolds number 1.6×10^5 was used in calculations with a Mach number of 0.046. The attack angle used was between 0° to 25° for cases of increase and decrease from the horizontal position of the airfoil.

3. Governing Equations and Boundary Conditions

The fluid was assumed to be steady state and incompressible with constant physical properties. Fluid flow was considered to be turbulent flow. The governing equations used to solve this case include:
The continuity equation:

$$\frac{\partial u}{\partial x}+\frac{\partial v}{\partial y}=0 \quad (1)$$

The momentum equation:

$$\rho\vec{u}+\vec{\nabla}\cdot(\rho\vec{u}\vec{u})=-\vec{\nabla}p+\vec{\nabla}\cdot\left(\vec{\vec{\tau}}\right)+\rho\vec{g}+\vec{F} \quad (2)$$

where ρ is fluid density, P is static pressure, $\vec{\vec{\tau}}$ is stress tensor, and $\rho\vec{g}$ and $\vec{F}$ are gravitational and external forces, respectively.
The boundary conditions for all surfaces are described as follows:

- In the inlet

$$u=u_{\infty}\cos\alpha,\ v=u_{\infty}\sin\alpha \quad (3)$$

- In the outlet

$$\frac{\partial u}{\partial x}=\frac{\partial v}{\partial x}=0 \quad (4)$$

- On the airfoil surface

$$u = v = 0 \quad (5)$$

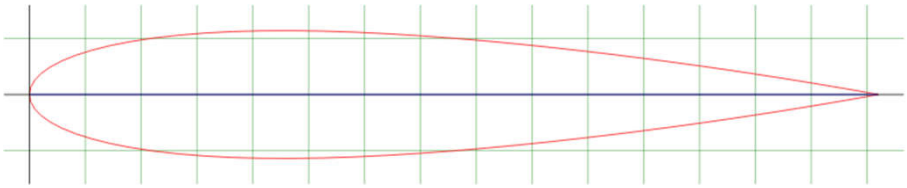

Figure 1. Geometry of NACA 0015 airfoil profile [12]

4. NUMERICAL METHOD

To solve the problem in a two-dimensional numerical simulation of this study, several assumptions were applied; namely, steady 2D flow, turbulent flow with Re = $1.6\text{x}10^5$, and fluid were considered as incompressible.

4.1. Grid Generation

Computational domain geometry was made in the form of a semicircular front and a rectangular back. The computational domain was made with the radius of a semicircular part of 50°C, the width and height of the rectangular sections of 50°C and 100°C, respectively, where C is the chord length of the airfoil as described in Figure 2.

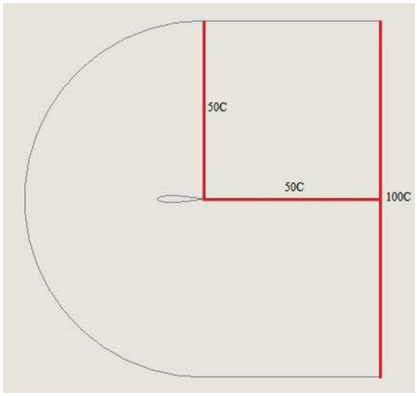

Figure 2. Geometry of computational domain

The type of grid used was C structured grid. The grid near the airfoil was closed to meet the turbulent model requirements [11]. The overall grid structure can be seen in Figure 3 and the grid structure close to the airfoil surface can be seen in Figure 4. The independent grid test was performed to obtain the minimum grid number, where the addition of the grid number will not affect the calculated parameters

[11]. From the independent grid test, it was found that the number of grids needed in this simulation was 116,000 as denoted in Table 1.

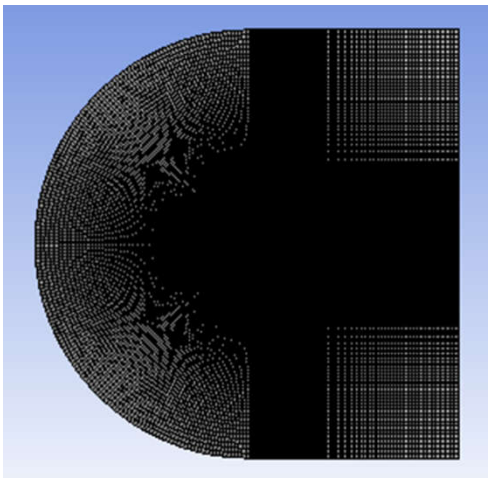

Figure 3. Grid structure of the computational domain

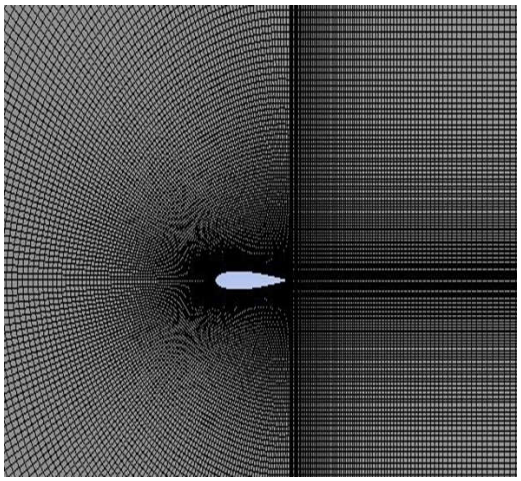

Figure 4.Grid structure near the airfoil

Table 1. Grid independent test

Number of grid	C_D (present simulation)	C_D (Ahmadi et al. [7])
47,950	0.0247	0.033
79,250	0.0268	
116,000	0.0282	
161,150	0.0283	

4.2. Turbulent Model

The turbulent model used in this numerical simulation was the *k-ε* standard with the standard wall function. Pressure-velocity coupling was solved by the SIMPLEC algorithm. The momentum equation was discretized by the upwind second order scheme, while the turbulent kinetic energy equation and dissipation ratio were discretized by the first order upwind scheme. The convergence criteria used were 10^{-5} for momentum equations, turbulent kinetic energy, and dissipation ratio.

5. Results and Discussion

5.1. Verification

To obtain accurate simulation results, the current numerical simulation results were compared with the experimental results of Ahmadi-Baloutaki et al. [7]. The equations used in calculating the aerodynamic coefficient of an airfoil are as follows:

Lift coefficient:

$$C_L = \frac{F_L}{0.5\rho U_\infty^2 C} \tag{6}$$

Drag coefficient:

$$C_D = \frac{F_D}{0.5\rho U_\infty^2 C} \tag{7}$$

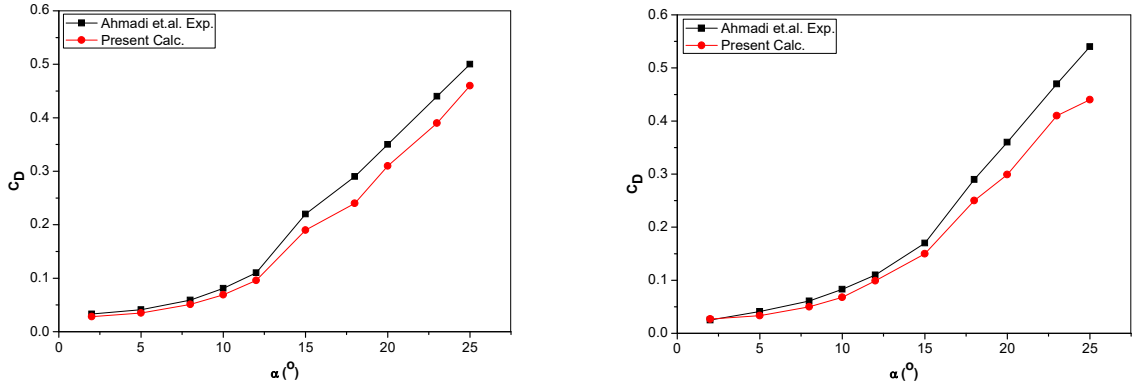

(a) (b)

Figure 5. Comparison of drag coefficient between simulation and experiment results in increasing attack angle for turbulent intensity (TI) of (a) 0.5% and (b) 4.6%

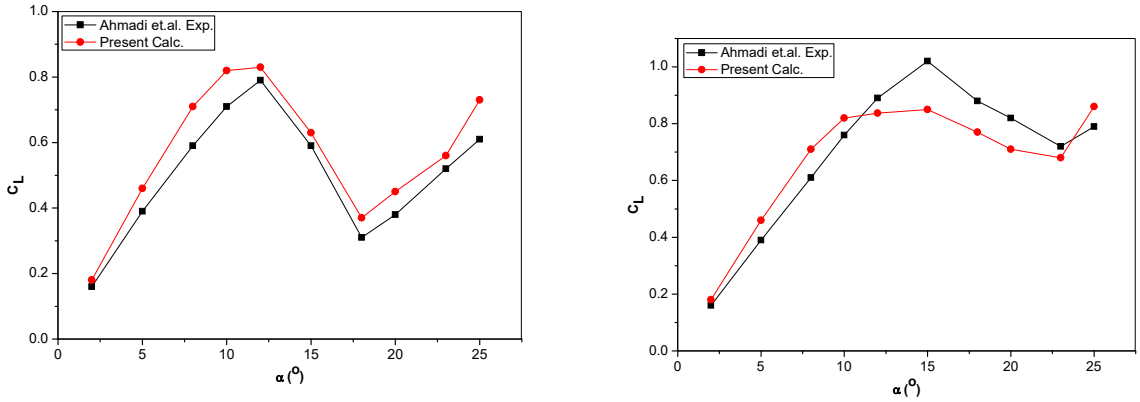

(a) (b)

Figure 6. Comparison of lift coefficient between simulation and experiment results in increasing attack angle for turbulent intensity (TI) of (a) 0.5% and (b) 4.6%

Figure 5 illustrates the comparison of the drag coefficients between the results of the present simulation and the experimental results of Ahmadi et al. (2015) [7]. The drag coefficient of the simulation results shows an agreement with that of the Ahmadi's et al. experiment. From Figure 5, it is found that the drag coefficient increases with increasing the attack angle at both turbulent intensities of 0.5% and 4.6%. A sharp increase in drag coefficient is observed with an increase in the attack angle for both turbulent intensities. As with the drag coefficient, the predicted coefficient of lift is observed as an agreement with the experimental results of Ahmadi et al. on increasing the attack angle as can be seen in Figure 6. The lift coefficient reaches the maximum value at the attack angle of 12° with the turbulent intensity of 0.5% and reaches the minimum value at the attack angle of 18°. At 4.6% turbulent intensity, the maximum value of the lift coefficient shifts at the attack angle 15° and the minimum value is found at the attack angle 23°.

5.2. Aerodynamic Performance

This aerodynamic performance is analyzed by considering the ratio of the lift force and the drag force to the increase in the attack angle as shown in Figure 7. As found in Figure 6, an increase in turbulent intensity results in a delay in stall condition as investigated by Ahmadi et al. [7]. From Figure 7 it is known that the higher turbulent intensity can increase the ratio of lift force and drag force (L/D) which

indicates higher aerodynamic performance on the profile of the NACA 0015 airfoil. Increasing the ratio of lift force and drag force (L/D) due to the increase in turbulent intensity on static airfoils is in accordance with the statements from Maldonado et al (2015) [8] and Kim and Xie (2016) [12].

5.3. Velocity Streamline

The effect of free-stream turbulence on the trailing edge vortex can be observed through velocity streamline. Figure 8 shows the process of forming a trailing edge vortex seen from a velocity streamline. From Figure 8, it is known that an increase in turbulent intensity can affect the process of forming the trailing edge vortex.

Vortex begins to form at the 15° attack angle with a turbulent intensity of 0.5%. This can be observed with the secondary flow above the airfoil surface, however, the vortex still does not completely cover the airfoil surface. This vortex is called the leading edge vortex (LEV) because the direction of rotation is from the leading edge and clockwise (Prangemeier, 2010) [13]. This condition indicates the start of the stall condition indicated by the decrease in the coefficient of lift. The vortex continues to develop and the second vortex appears around the trailing edge of the airfoil from the 18° attack angle. This second vortex is called trailing edge vortex (TEV) because the direction of rotation is counterclockwise. Both of these vortices continue to grow until the 25° attack angle. At the 15° attack angle with a turbulent intensity of 4.6%, the vortex formed is relatively small compared to that of the turbulent intensity of 0.5%. The vortex begins to increase at the 18° attack angle but has not completely covered the airfoil surface. This causes the stall process to start which is indicated by the decrease in the coefficient of lift. The stall process can occur because of the flow separation which results in the formation of a vortex. The vortex continues to develop until a TEV is formed from the 23° to the 25° attack angles. However, LEV starts to disappear at the 25° attack angle.

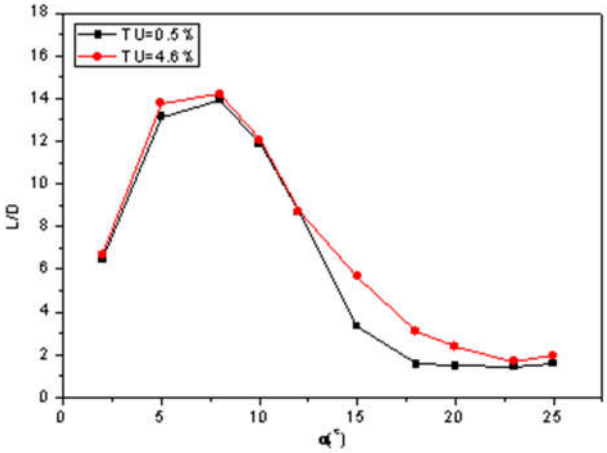

Figure 7. Effect of turbulent intensity on ratio of lift force and drag force in increase of attack angles

From the streamline, it can be seen that the process of forming a vortex is different in the increasing angle of attack. The higher the attack angle is, the greater the separation of flow. Flow separation can affect the process of vortex formation. From the streamline, it can be seen that the process of vortex formation is different from variations in turbulent intensity. The process of vortex formation is delayed at 4.6% turbulent intensity. At the 15° and -15° attack angles with a turbulent intensity of 0.5%, the vortex diameter formed is quite large, while the turbulent intensity of 4.6% vortex begins to form with a smaller diameter. The second vortex begins to form at the attack angles of 18° and -18° with the turbulent intensity of 0.5%, while the second vortex formed at the 23° attack angle at turbulent intensity of 4.6% as it is revealed by Leu et al. (20120 [14].

5.4. Vorticity

The increased turbulent intensity in the free stream region can affect vorticity. Comparison of growth and magnitude of vorticity with the turbulent intensity of 0.5% and 4.6% is shown in Figure 9. Vorticity at the trailing edge begins to form for the 18° attack angle with a turbulent intensity of 0.5%. This is indicated by the presence of vorticity that rolls in a circle on the trailing edge region. Vorticity on the trailing edge area has a negative value which indicates that the vorticity has a counterclockwise rotation (Prengemeier et al., 2010) [13] and (Panda and Zaman, 1994) [15]. The vorticity continues to develop until the 25° attack angle with different strengths. At the turbulent intensity of 4.6%, vorticity at the trailing edge region is observed at the attack angle 23°.

6. Conclusions

Investigation of interactions between free-stream turbulence against the trailing edge vortex through two-dimensional numerical simulations has been carried out. Comparisons have been made to the profile of the NACA 0015 airfoil for the Reynolds number 1.6 x 10^5 with 2° and 25° attack angles at0.5% and 4.6% turbulent intensity. From the results of numerical simulations, it was found that verification has shown an agreement between the results of the simulation and the experimental results. The increase of turbulent intensity can improve aerodynamic performance characterized by static stall delay. Increased turbulent intensity also delayed the process of forming the trailing edge vortex.

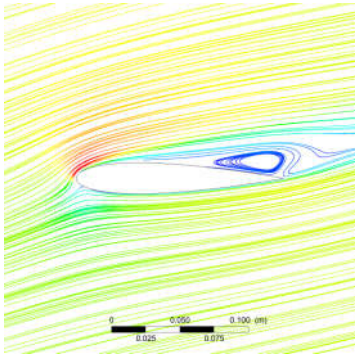

α = 15°, TI = 0.5%

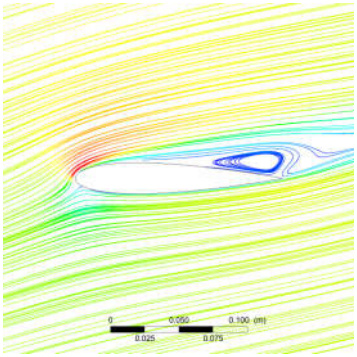

α = 15°, TI = 4.6%

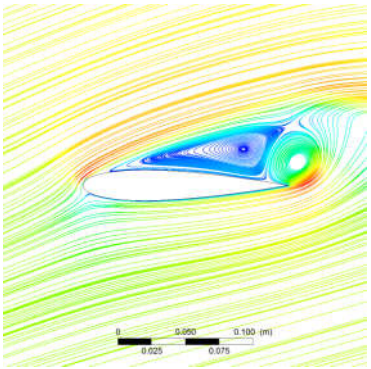

α = 18°, TI = 0.5%

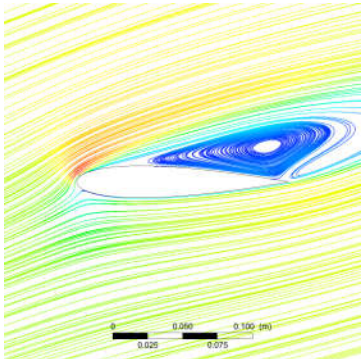

α = 18°, TI = 4.6%

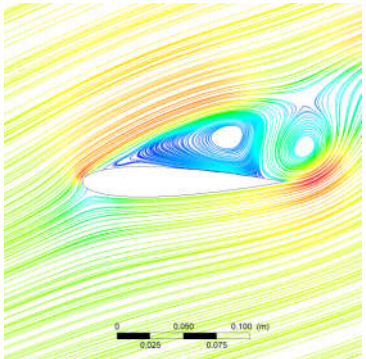

α = 20°, TI = 0.5%

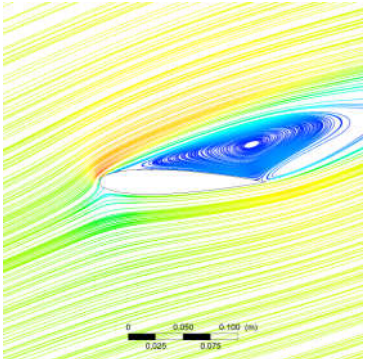

α = 20°, TI = 4.6%

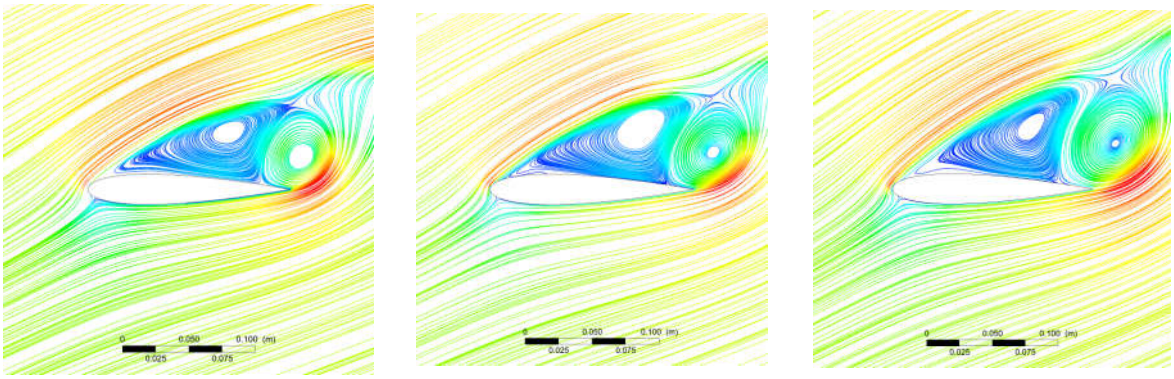

α = 23°, TI = 0.5% α = 23°, TI = 4.6% α = 25°, TI = 0.5%

α = 25°, TI = 4.6%

Figure 8. Velocity streamline for variation of attack angles at turbulent intensities of 0.5% and 4.6%

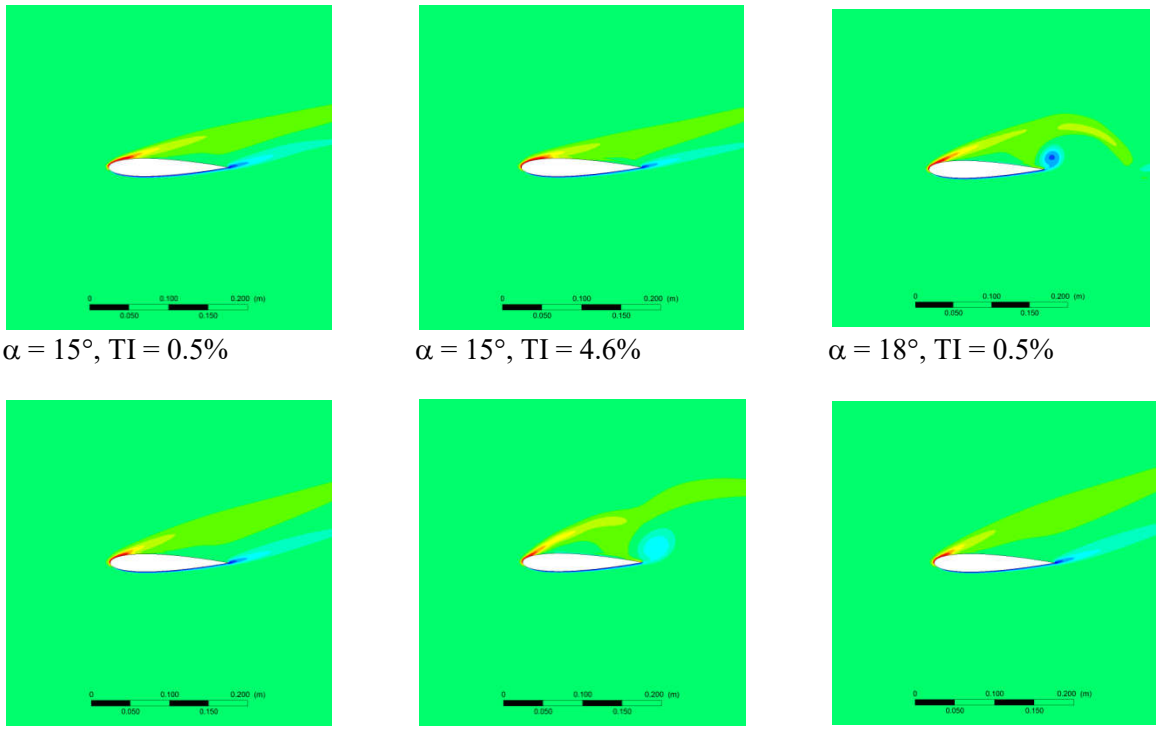

α = 15°, TI = 0.5% α = 15°, TI = 4.6% α = 18°, TI = 0.5%

α = 18°, TI = 4.6% α = 20°, TI = 0.5% α = 20°, TI = 4.6%

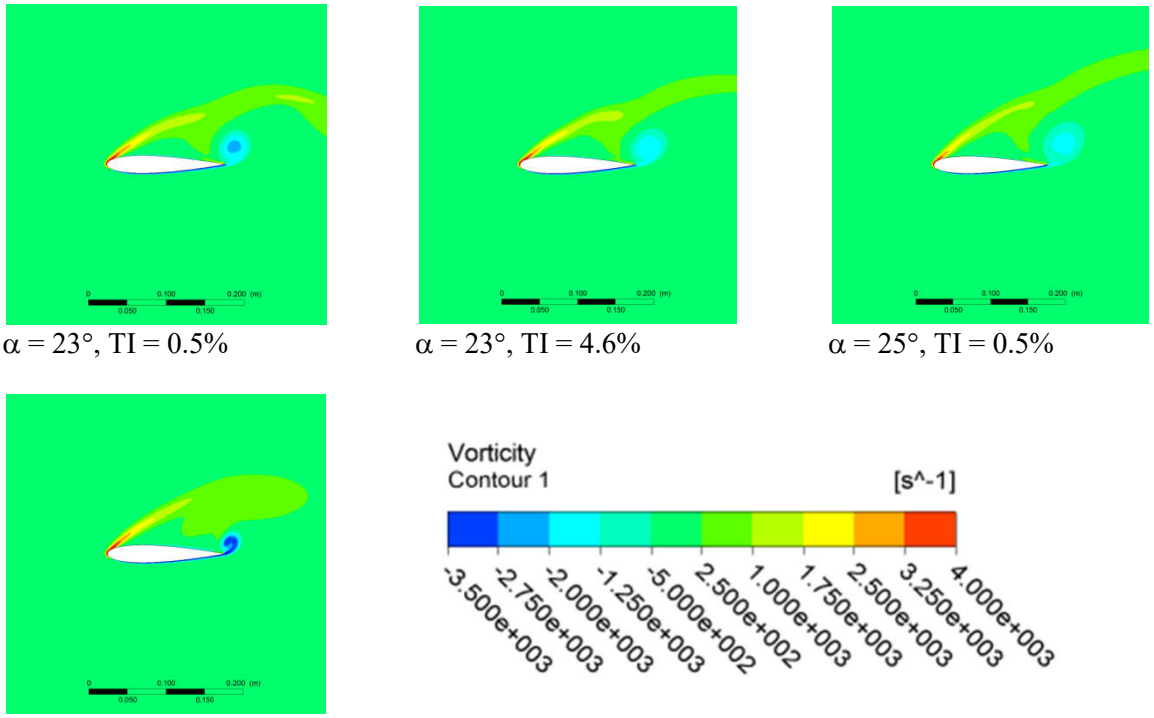

α = 23°, TI = 0.5% α = 23°, TI = 4.6% α = 25°, TI = 0.5%

α = 25°, TI = 4.6%

Figure 9. Vorticity for variation of attack angles at turbulent intensities of 0.5% and 4.6%

Acknowledgements
This work was supported by the Faculty of Engineering, Diponegoro University (DIPA FT 2019). The authors are grateful to all research members, especially Thermofluid Lab. and Energy Conversion Lab. of Mechanical Engineering of Diponegoro University.

References

[1] Ministry of Energy and Mineral Resources 2016 to 2030 World Energy Demand Increases 45% http://www.esdm.go.id/berita/37-umum
[2] Çengel YA, and Cimbala JM 2006 *Fluid Mechanics: Fundamentals and Applications* 1)Ed 2006 New York: McGraw-Hill
[3] Şahin İ., and Acir A 2015 Numerical and experimental investigations of lift and drag performances of NACA 0015 wind turbine airfoil *IJMMM* **3** 22-25.
[4] Qing'an Li, Jianzhong Xu, Takao Maeda, Yasunari Kamada, Shogo Nishimura, Guangxing Wu, and Chang Cai 2019 Laser doppler velocimetry (LDV) measurements of airfoil surface flow on a Horizontal Axis Wind Turbine in boundary layer *Energy* **183** 341-357.
[5] Kobra Gharali, Eshagh Gharaei, M. Soltani, and Kaamran Raahemifar 2018 Reduced frequency effects on combined oscillations, angle of attack and free stream oscillations, for a wind turbine blade element *Renewable Energy* **115** 252-259
[6] Giuni M., and Green R.B 2013 Vortex formation on squared and rounded tip *Aerospace Science and Technology* 29 191-199.
[7] Ahmadi-Baloutaki M., Carriveau R., and Ting D.S.K 2015 An experimental study on the interaction between free-stream turbulence and a wing-tip vortex in the near-field *Aerospace Science and Technology* **43** 395-405
[8] Maldonado V., Castillo L., Thormann A., and Meneveau C 2015 The role of free stream turbulence with large integral scale on the aerodynamic performance of an experimental low reynolds number S809 wind turbine blade *Journal of Wind Engineering and Industrial Aerodynamics* **142** 246-257

[9] Qing'an Li, Yasunari Kamada, Takao Maeda, Yusuke Nishida 2017 Experimental investigations of boundary layer impact on the airfoil aerodynamic forces of Horizontal Axis Wind Turbine in turbulent inflows *Energy* **135** 799-810.
[10] Yusik Kim and Zheng-Tong Xie 2016 Modelling the effect of freestream turbulence on dynamic stall of wind turbine blades *Computers and Fluids* **129** 53-66.
[11] Yao J., Yuan W., Wang J., Xie J., Zhou H., Peng M., and Sun Y 2012 Numerical simulation of aerodynamic performance for two dimensional wind turbine airfoils *Procedia Engineering* **31** 80-86
[12] Kim Ya, and Xie Z.T 2016 Modelling the effect of freestream turbulence on dynamic stall of wind turbine blades *Computers & Fluids* **129** 53-66.
[13] Prangemeier T., Rival D., and Tropea C 2010 The manipulation of trailing-edge vortices for an airfoil in plunging motion *Journal of Fluids and Structures* **26** 193-204
[14] Leu T.S., Yu J.M., Hu C.C., Miau J.J., Liang S.Y., Li J.Y., Cheng J.C., and Chen S.J 2012 Experimental study of free stream turbulent effects on dynamic stall of pitching airfoil by using particle image velocimetry *AMM* **225** 103-108
[15] Panda J., and Zaman K.B.M.Q 1994 Experimental investigation of the flow field of an oscillating airfoil and estimation of lift from wake surveys *Journal of Fluid Mechanics* **265** 65.